The first airborne comparison of N_2O_5 measurements over the UK using a CIMS and BBCEAS during the RONOCO campaign

Michael Le Breton[1], Asan Bacak[1], Jennifer B.A. Muller[1], Thomas. J. Bannan[1], Oliver Kennedy[3], Bin Ouyang[3], Ping Xiao[2], Stéphane J.-B. Bauguitte[4], Dudley E. Shallcross[2], Roderic L. Jones[3], Mark J.S. Daniels[5], Stephen M. Ball[5] and Carl J. Percival[1]*

[1]*The Centre for Atmospheric Science, The School of Earth, Atmospheric and Environmental Sciences, The University of Manchester, Simon Building, Brunswick Street, Manchester, M13 9PL, UK.*

[2]*School of Chemistry, The University of Bristol, Cantock's Close BS8 1TS, UK.*

[3]*Department of Chemistry, University of Cambridge, Cambridgeshire, CB2 9EW, UK*

[4]*Facility for Airborne Atmospheric Measurements (FAAM), Building 125, Cranfield University, Cranfield, Bedford, MK43 0AL, UK*

[5]*Department of Chemistry, University of Leicester, University Road, Leicester, LE1 7RH, UK*

[*]*Corresponding author Email: carl.percival@manchester.ac.uk*

Abstract

Dinitrogen pentoxide (N_2O_5) plays a central role in nighttime tropospheric chemistry as its formation and subsequent loss in sink processes limits the potential for tropospheric photochemistry to generate ozone the next day. Since accurate observational data for N_2O_5 are critical to examine our understanding of this chemistry, it is vital also to evaluate the capabilities of N_2O_5 measurement techniques through the co-deployment of the available instrumentation. This work compares measurements of N_2O_5 from two aircraft instruments onboard the Facility for Airborne Atmospheric Measurements (FAAM) BAe-146 aircraft during the Role of Nighttime Chemistry in Controlling the Oxidising Capacity of the

Atmosphere (RONOCO) measurement campaigns over the United Kingdom in 2010 and 2011. A chemical ionisation mass spectrometer (CIMS), deployed for the first time for ambient N_2O_5 detection during RONOCO, measured N_2O_5 directly using I^- ionisation chemistry and an aircraft-based broadband cavity enhanced absorption spectrometer (BBCEAS), developed specifically for RONOCO, measured N_2O_5 by thermally dissociating N_2O_5 and quantifying the resultant NO_3 spectroscopically within a high finesse optical cavity.

N_2O_5 mixing ratios were simultaneously measured at 1 second time resolution (1 Hz) by the two instruments for 8 flights during RONOCO. The sensitivity for the CIMS instrument was 52 ion counts $pptv^{-1}$ with a limit of detection of 7.4 pptv for 1 Hz measurements. BBCEAS, a proven technique for N_2O_5 measurement, had a limit of detection of 2 pptv. Comparison of the observed N_2O_5 mixing ratios show excellent agreement between the CIMS and BBCEAS methods for the whole dataset, as indicated by the square of the linear correlation coefficient, $R^2 = 0.89$. Even stronger correlations (R^2 values up to 0.98) were found for individual flights. Altitudinal profiles of N_2O_5 obtained by CIMS and BBCEAS also showed close agreement ($R^2 = 0.93$). Similarly, N_2O_5 mixing ratios from both instruments were greatest within pollution plumes and were strongly positively correlated with the NO_2 concentrations. The transition from day to night time chemistry was observed during a dusk-to-dawn flight during the summer 2011 RONOCO campaign: the CIMS and BBCEAS instruments simultaneously detected the increasing N_2O_5 concentrations after sunset. The performance of the CIMS and BBCEAS techniques demonstrated in the RONOCO dataset illustrate the benefits that accurate, high-frequency, aircraft-based measurements have for improving understanding the nighttime chemistry of N_2O_5.

1. Introduction

Dinitrogen pentoxide (N_2O_5) is an important nighttime oxide of nitrogen in both the stratosphere and troposphere.[1,2] Nighttime production of N_2O_5 has a significant impact on the lifetime of NO_x, enabling N_2O_5 to act as a nighttime sink of NO_x or a reversible storage of NO_x allowing possible transport.[3] Furthermore, it also has a major impact on the formation of NO_3, the main tropospheric nighttime oxidant. Formation of N_2O_5 in the stratosphere limits

ozone (O_3) production[4] and its presence in the troposphere enables halogen activation and the production of inorganic nitrate[5] by reaction with salt aerosols, forming $ClNO_2$.[6] The efficiency of daytime tropospheric O_3 production and the formation of secondary aerosols are affected by nitrate radical (NO_3) and N_2O_5 levels the previous night[7] NO_3 initiates the processing of anthropogenic and biogenic emissions at nighttime and has been shown to compete effectively with the daytime hydroxyl radical processing, especially for unsaturated volatile organic compounds (VOC) due to their high reactivity with NO_3.[8] To improve the understanding of the processes affecting O_3 formation and air quality, it is necessary to improve the understanding of the atmospheric cycle of N_2O_5 and NO_3 through its formation, loss, spatial variability and role in the regulation of NO_x and budgets of VOCs.[9]

NO_3 is formed through the reaction of O_3 and NO_2, which can then further react with NO_2 to form N_2O_5. N_2O_5 is in thermal equilibrium with NO_3 which is typically established in a few minutes in the atmosphere.[10]

$$NO + O_3 \rightarrow NO_2 + O_2 \qquad \text{R1}$$

$$NO_2 + O_3 \rightarrow NO_3 + O_2 \qquad \text{R2}$$

$$NO_2 + NO_3 + M \rightleftarrows N_2O_5 + M \qquad \text{R3}$$

NO_3 and its equilibrium partner N_2O_5 are only abundant at night due to the rapid daytime photolysis of NO_3; j (NO_3) will vary during the day, season and latitude of course but a typical daytime value is (0.2 s^{-1}).[11] NO_3 and N_2O_5 are also suppressed in the presence of fresh pollution sources because NO_3 undergoes a fast reaction with NO. N_2O_5 mixing ratios can build up during the night reaching maximum concentrations of a few ppbv.[12,13]

N_2O_5 acts as a sink for NO_x in the troposphere through its reaction with water to produce nitric acid (HNO_3).[14,15]

$$N_2O_5 + H_2O_{het} \rightarrow 2HNO_3 \qquad \text{R4}$$

Therefore, the nighttime oxidative capacity of the troposphere and NO_3 availability is partially dependent upon the hydrolysis of N_2O_5. The removal of NO_3 and N_2O_5 via reaction (4) directly impacts the production of daytime oxidants such as OH and O_3. The relationship between NO_x availability and tropospheric O_3 production rates is complex, but the hydrolysis of N_2O_5 is thought to decrease O_3 concentrations in low NO_x conditions and increase O_3 in high NO_x regions.[16,17]

N_2O_5 also affects the tropospheric aerosol budget as the nitric acid produced, via its hydrolysis, partitions to the aerosol phase at low temperatures or in regions of excess ammonia.[18,19] N_2O_5 can also be directly taken up on particles or fog droplets resulting in a production of dissolved nitrate.[20] The aerosol budget is a significant area of uncertainty[21] and its impact on regional air quality and climate is difficult to quantify.[22-24] Additionally, the uptake co-efficient for N_2O_5 is rather variable, depending on aerosol composition and meteorological conditions.[25,26] Recent studies have shown heterogeneous chemistry of N_2O_5 on chloride containing aerosols efficiently releases chlorine radicals to the atmosphere via the formation and subsequent photolysis of $ClNO_2$.[6]

The first measurements of NO_3 in the troposphere using differential optical absorption spectroscopy DOAS[27] were followed by a wide range of ground-based studies investigating the role of NO_3 in polluted and clean tropospheric environments.[28,29] The measurement of N_2O_5 during these DOAS studies was not possible as it does not absorb at any convenient wavelengths. Techniques for measuring NO_3 were then adapted to infer N_2O_5 concentrations by forcing the thermal equilibrium between NO_3 and N_2O_5 to favour the detectable NO_3 species. Optical absorption within high-finesse cavity techniques[30,31], ionisation mass spectrometry[32] or laser induced fluorescence (LIF) have all been used to detect the NO_3 produced from the thermal dissociation of N_2O_5.[33,34] Previous in situ measurements indicate an instrument with a fast time response as achieved by Dorn *et al.* (2013)[35] with an integration time of 0.2 to 0.5 ppt, is necessary to capture temporal variability of NO_3 and (N_2O_5)[36, 25] however there are only a few techniques with this capability. Kennedy *et al.* (2011)[13] report measurements of N_2O_5 via the thermal dissociation of N_2O_5 on a second channel of a broadband cavity enhanced absorption spectrometer (BBCEAS) onboard the FAAM BAe-146 aircraft during the RONOCO campaign. In this paper, N_2O_5 detection using

a chemical ionisation mass spectrometer is compared with the BBCEAS technique using measurement data obtained during the RONOCO project.

2. Experiment details

2.1. BBCEAS instrument

Cavity enhanced absorption spectroscopy with broadband light sources was first demonstrated with arc lamps by Fiedler *et al.* (2003)[37] and light emitting diodes (LEDs) by Ball et al (2004). In the intervening 10 years, many groups have developed broadband cavity-based spectrometers targeting species of atmospheric interest both in laboratory experiments and field work.[38-43] The LED broadband cavity enhanced absorption spectrometer used for RONOCO provides NO_3, N_2O_5 and NO_2 measurements using three separate channels, each with their own LED light source, cavity and grating spectrometer. The instrument has been described in detail by Kennedy *et al.* (2011)[13] and builds on our previous work measuring NO_3 and N_2O_5 by BBCEAS in the marine boundary layer[44] and the polluted urban atmosphere.[45]

Briefly, channels 1 and 2 of the BBCEAS instrument operated at red wavelengths to target N_2O_5 and NO_3 respectively, and channel 3 operated at blue wavelengths to target NO_2. The BBCEAS instrument sampled air through two rear facing inlets situated on the fuselage of the FAAM BAe-146 aircraft. The flow through the first inlet (50 litres per minute) was divided between channels 1 and 2. Prior to entering the cavity of channel 1, the air flow passed through a preheater at 120°C to thermally decompose N_2O_5 in the sample into NO_3 and NO_2 with an efficiency of >99.6% for the range of inlet air temperatures and NO_2 mixing ratios encountered during RONOCO flights. The NO_3 produced from N_2O_5 decomposition, plus any ambient NO_3, was quantified via the 662 nm absorption band of NO_3 inside the cavity of channel 1. The cavity was held at 80°C to prevent the recombination of NO_3 with NO_2. The same 662 nm absorption band was used to measure ambient NO_3 in channel 2, the cavity of which was maintained close to the air temperature outside the aircraft in order to minimise any perturbation of the NO_3/ N_2O_5 equilibrium. This thermal stabilisation was achieved by flowing ambient air sampled through the instrument's second inlet through a sheath surrounding the cavity. The N_2O_5 concentration was thus calculated from the difference

between the NO_3 signals recorded in the heated and ambient temperature cavities. The concentrations of N_2O_5 and NO_3 were corrected for the measured losses of these species in the inlet and on the walls of channels 1 and 2.

The gas flow exhausted from the cavity of channel 2 was then passed into the cavity of channel 3 wherein NO_2 was quantified via its highly-structured absorption features between 440 and 480 nm. Excellent agreement was obtained between the NO_2 measurements from the BBCEAS instrument and from a commercial, photolytic converter chemiluminescence (CL) detector on board the FAAM BAe-146 aircraft[1]. Typical 1σ detection limits of the BBCEAS instrument were 2.4 pptv for N_2O_5 and 1 pptv for NO_3 (1 s measurements), and 10 pptv for NO_2 (10 s measurements).

2.2. CIMS instrument

The CIMS technique has been implemented for field measurements of gaseous species since the detection of H_2SO_4 in 1991.[46] Following this work, CIMS has been further developed to successfully detect a wide range of gaseous species using a number of different ionisation schemes. This development of CIMS and the advances made in the technology have been reviewed by Huey (2006).[47] Here, the development and implementation of CIMS to detect N_2O_5 is presented and compared to BBCEAS. The CIMS instrument deployed during RONOCO was built by the Georgia Institute of Technology as previously described by Nowak *et al*. (2007)[48] and Le Breton *et al*. (2012).[49] The schematic in figure 1 shows the set up used and operating conditions of the CIMS on board the airborne platform FAAM BAe-146 research aircraft.

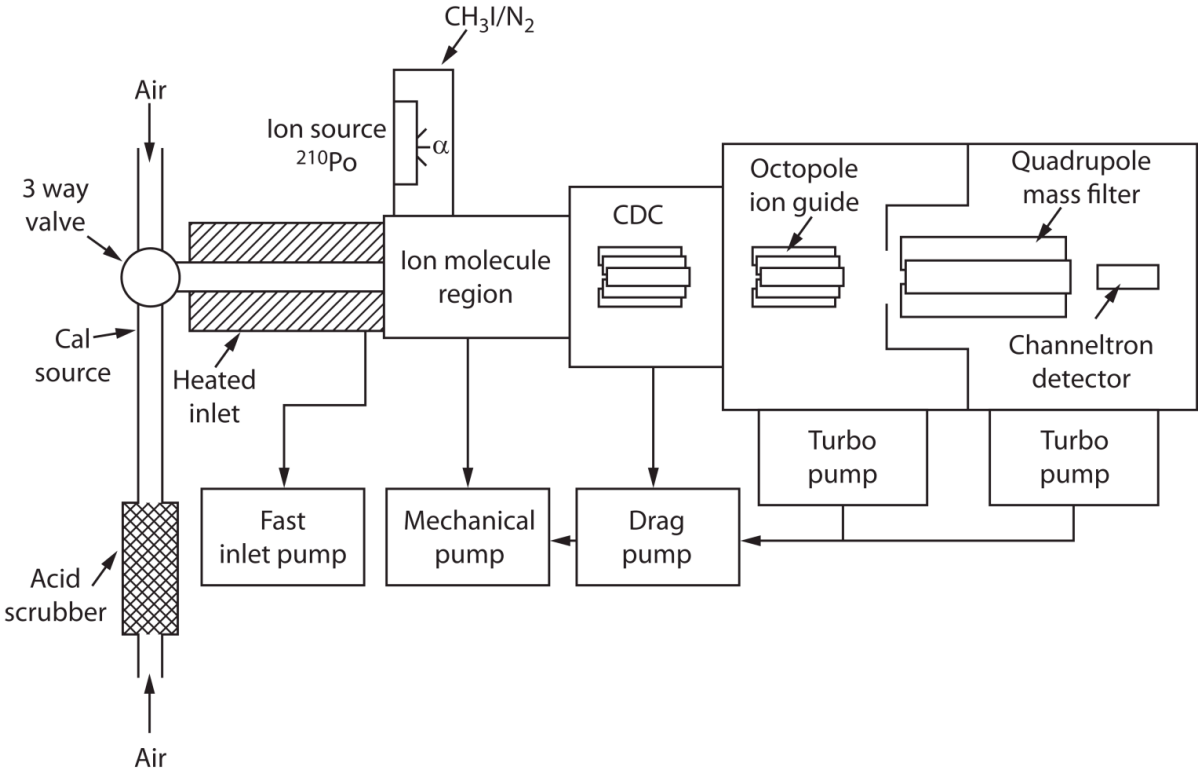

Figure 1. Schematic of chemical ionisation mass spectrometer (CIMS) used in this study. Arrows indicate direction of gas flow. Dimensions are not to scale.

2.2.1. Inlet and ionisation

The CIMS is fitted with two identical inlets, one for background measurements and one for sampling. They consist of 6 cm OD diameter PFA tubing of length 580 mm and are heated to 50°C to reduce surface loss. A 3-way valve is used to automate switching between measuring the ambient atmospheric air and the background line which passes the ambient air through and acid scrubber, removing all acids and N_2O_5 from the flow.[49,50] An orifice of diameter 0.9 mm was positioned at the front of the inlet to restrict the flow to 5.8 SLM which was brought in using a rotary vane pump (Picolino VTE-3, Gardner Denver Thomas). This corresponded to a residence time of 0.28 s at standard temperature and pressure in the total length of the inlet tubing.

The pressure in the ion molecule region (IMR) was maintained at 19 Torr throughout the flight and was controlled and measured using a mass flow controller (MKS 1179 and MKS M100 Mass flow controllers, MKS Instruments, UK) and Baratron (1000 Torr range,

Pressure Transducer, Model No. 722A, MKS Instruments, UK) and a dry scroll pump (UL-DISL 100, ULVAC Industrial). Here, N_2 and the ionisation gas mixture of $CH_3I/H_2O/N_2$ at a rate of 1 standard cubic centimetres (SCCM) passed over the ion source (Polonium-210 inline ioniser, NRD inc Static Solutions Limited) producing an excess of I^- and $I^-.H_2O$ ions in the ion molecule region (IMR) as described in Le Breton *et al*. (2012).[49] These reagent ions then allow the species of interest in the air sample to be detected.

2.2.2. Ion filtration and detection

The ions then passed through a pinhole of a charged plate, which entered the mass spectrometer section of the instrument, i.e. the first octopole ion guide chamber which is the collisional dissociation chamber (CDC). Here, weakly-bound ion-water clusters are broken up to simplify the resultant mass spectrum. Inside the CDC, the pressure was 0.25 Torr and the local electric field divided by the gas number density (E/N) was 180 Townsend (Td = 10^{-17} V cm^2). The pressure in the CDC of less than 1 Torr was achieved by the use of a molecular drag pump (MDP-5011, Adixen Alcatel Vacuum Technology). After the CDC, the ions passed through the second octopole ion guide, which has the effect of collimating the ions. The octopole chamber was held at a pressure of 10^{-3} Torr which was maintained by a turbomolecular pump (V-81M Navigator, Varian Inc. Vacuum Technologies). Beyond the second octopole chamber, the ions were mass selected by a quadrupole with pre and post filters with entrance and exit lenses (Tri-filter Quadrupole Mass Filter, Extrel CMS).

The quadrupole section was kept at a pressure of 10^{-4} Torr by a second 15 turbomolecular pump (V-81M Navigator, Varian Inc. Vacuum Technologies). The selected ions were then detected and counted by a continuous dynode electron multiplier (7550M detector, ITT Power Solutions, Inc.).

2.2.3 Ionisation scheme

The ion-molecule chemistry using iodide ions (I^-) for trace gas detection has been described by Slusher *et al*. (2004)[32] and was utilised here to detect N_2O_5 and nitric acid (HNO_3). The heated inlet and lower electric field strength (25 V cm^2 compared with 180 V cm^2) allows the CIMS to detect NO_3 and N_2O_5 as NO_3^-. Here, a small peak is observed for the ion $N_2O_5^-$, although at a sensitivity ratio of 200:1 and therefore is negligible. Laboratory calibrations confirm an interference at mass 62 by NO_3 is not observed, deeming the system in this setup is unable to detect NO_3.

A gas mixture of methyl iodide (CH_3I) and H_2O in N_2 is used to obtain reagent ions I^- and water clusters $I^-.H_2O$. The mix was produced using a manifold by evaporating the liquid deionised H_2O and CH_3I sequentially into the manifold to reach the following partial pressures of 10 Torr H_2O and 15 Torr CH_3I. Nitrogen was then added up to 5 bar to make an ionisation gas mixture of 0.39 % CH_3I and 0.26 % H_2O. CH_3I (≥ 99.5 %) was purchased from Sigma Aldrich and used as provided.

N_2O_5 and HNO_3 were ionised by through the I^- ionisation scheme via reactions (5) and (6);

$$I^-.H_2O + N_2O_5 \rightarrow NO_3^- + NO_2 + I.H_2O \qquad \text{R5}$$

$$I^-.H_2O + HNO_3 \rightarrow HNO_3.I^- + NO_2 + H_2O \qquad \text{R6}$$

which enabled N_2O_5 to be detected selectively via the NO_3^- ion signal at *m/z* =62 and HNO_3 to form an adduct with I^- and be detected at *m/z* = 189 as shown in figure 2. Typical reagent ion count values were I^-= 1.5 ×10^6 Hz, and $I.H_2O^-$ = 2.5 ×10^6 Hz.

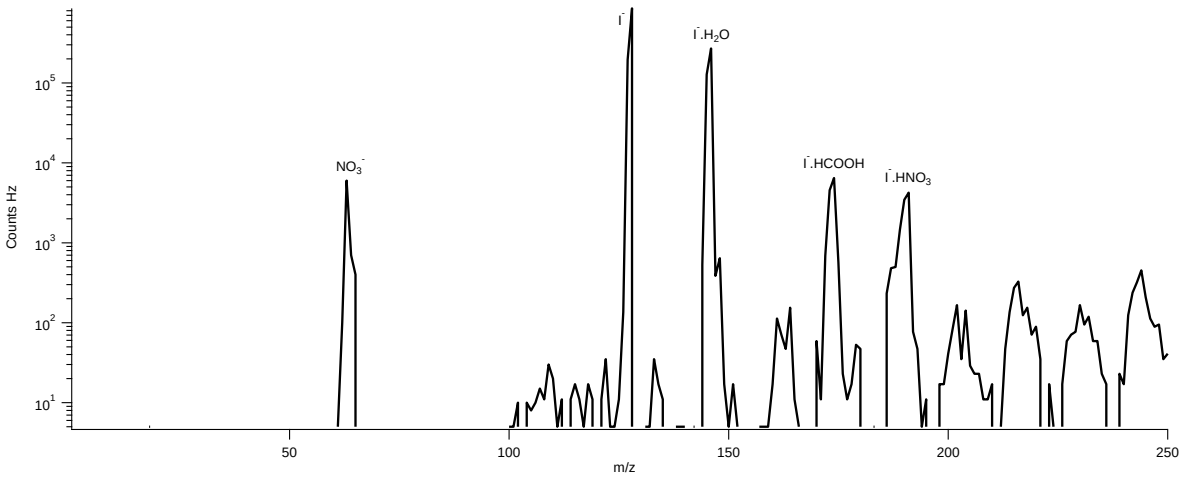

Figure 2. Mass spectrum of CIMS during flight B534 at 22:13. Ionisation peaks and N_2O_5 detected mass (at mass 62, NO_3) are labelled.

As the ionisation efficiency depends on the presence of water vapour through the production of $I^-.H_2O$,[32,50] water vapour was added to the ionisation gas mixture, so as to produce an excess of $I^-.H_2O$ cluster ions over the I^- ions and hence allow operation in the water vapour independent regime[32]. The dependency of CIMS sensitivity to $I.H_2O$ is shown in figure 3, presenting a formic acid calibration over a range of RH and therefore $I^-.H_2O$ counts. Mass 145 ($I^-.H_2O$) counts never fell below 150 000 during operation onboard the aircraft due to this addition of water vapour. Formic acid has been chosen as the reference mass due to the extensive development on this CIMS for detection and calibration of this species. The sensitivity of the CIMS for N_2O_5 is assumed to be independent of water vapour amounts, as laboratory tests have shown formic acid and N_2O_5 sensitivities are linear, as explained in detail in section 2.2.4.

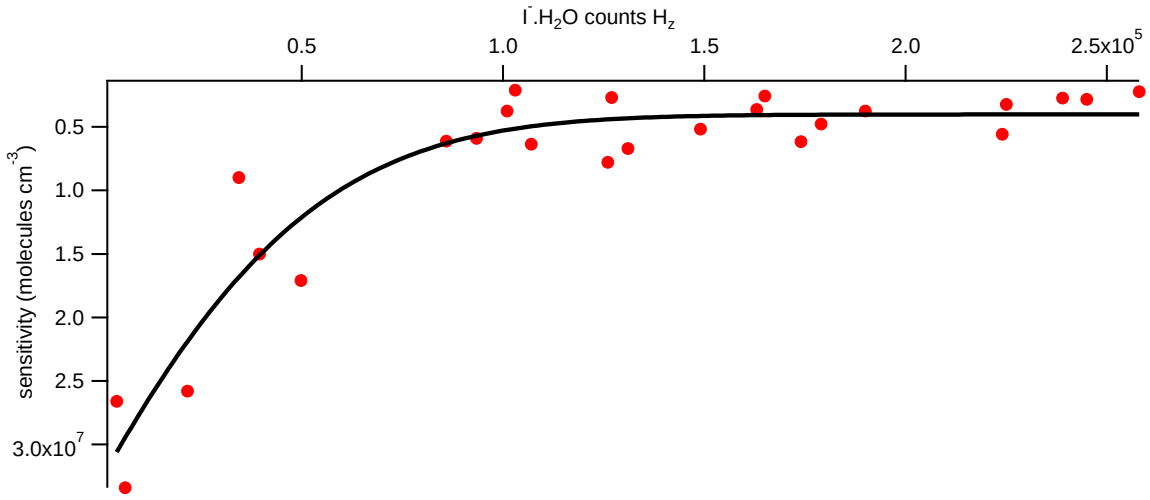

Figure 3. Formic acid calibration at a range of RH values, indicating that the sensitivity above 100 000 $I^-.H_2O$ counts is independent of $I.H_2O^-$ counts.

2.2.4. Calibrations

The CIMS was unable to be calibrated for N_2O_5 during the RONOCO campaign, therefore a single BBCEAS data point was taken to estimate sensitivity of the CIMS to N_2O_5. The formic acid calibration for this flight was then used to calculate the relative sensitivity ratio, allowing the campaigns formic acid calibrations to determine the CIMS sensitivity towards N_2O_5. Airborne formic acid calibrations have been well developed for operation of this CIMS and are performed in-flight and post flight as described in Le Breton *et al.* (2012, 2013).[49,50] N_2O_5 was calibrated in the laboratory after the campaign by producing a known concentration of N_2O_5 as described later and simultaneously calibrating the instrument for formic acid. A linear relationship was found for formic acid and N_2O_5 sensitivities. Figure 4 shows how the CIMS sensitivity to formic acid and N_2O_5 increase linearly.

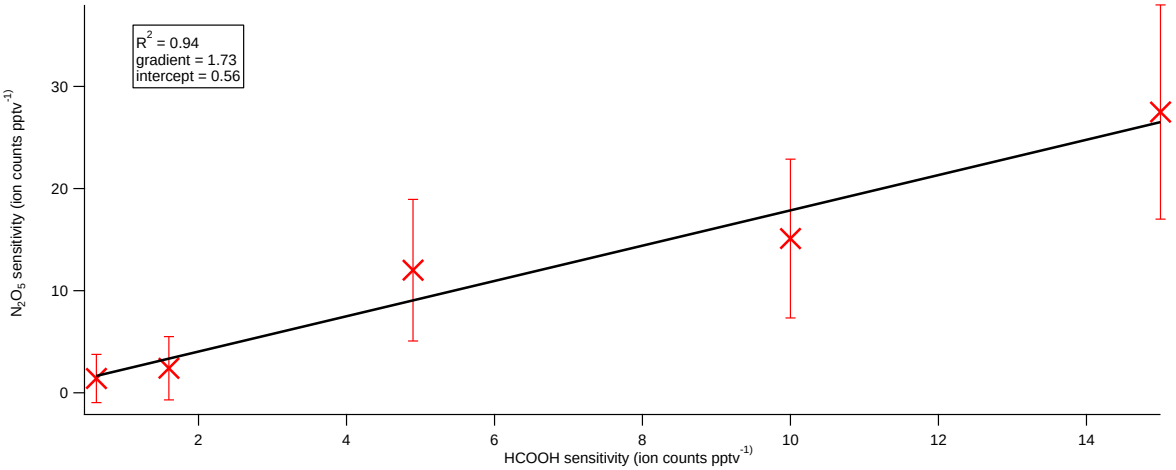

Figure 4. Formic acid and N_2O_5 laboratory calibration correlation. Error bars for N_2O_5 are represented by $2 \times \sqrt{[N_2O_5]}$.

N_2O_5 was produced by the reaction between NO_2 and O_3. O_3 was generated by allowing dried oxygen to flow through a silent discharge ozone generator (Argentox). Ozonised oxygen was allowed to flow through NO_2, frozen down in a Pyrex trap and warmed to room temperature at atmospheric pressure. The flow passed through a Pyrex mixing volume of 5 litres and a Pyrex trap held at 195 K to collect the N_2O_5 and any unreacted NO_2. As the first trap empties, the flow of ozonised oxygen is reversed and the second trap, now containing mostly N_2O_5 was allowed to warm, as the trap initially containing NO_2 is cooled to 195 K. The flow is reversed several times to purify the N_2O_5. Water vapour was excluded from the glassware by purging the system with O_3 and oxygen for ten minutes before use. The N_2O_5 collected was stored under vacuum at 77 K until used for calibrations.

The N_2O_5, maintained at 195K, was then introduced to the CIMS and detected at *m/z* 62. The inlet was split to allow a flow to be diverted to a NO_x analyser. As the inlet is heated, all N_2O_5 is thermally decomposed producing NO_2 and NO_3. The concentration of N_2O_5 is calculated assuming 100% efficiency of the heater to decompose the N_2O_5 to NO_2, detected by the NO_x analyser. The signal in the CIMS decreased to background count levels as soon as the inlet is heated, confirming full thermal decomposition of N_2O_5 and also no interference at this mass by NO_3.

2.3 FAAM BAe-146 onboard instruments

In addition to the N_2O_5 data from the BBCEAS and CIMS, NO_2 measurements are used in this analysis. Nitric oxide (NO) and nitrogen dioxide (NO_2) were measured using separate channels of a photolytic "blue light" converter chemiluminescence detector and were reported every 1 second with an uncertainty of ± 6% ppbv[51] Ozone was measured using a UV Photometric Ozone Analyser at 1 Hz with an uncertainty of 15 ±3 ppbv.[52] The FAAM core GPS-aided inertial Navigation system is also used to provide altitude, longitude and latitude.

2.4 RONOCO 2010 and 2011 campaign

The two RONOCO flying campaigns were conducted in July 2010 and January 2011 based at the East Midlands Airport, in central United Kingdom. The scientific objectives of RONOCO were to determine the spatio-temporal variation of tropospheric NO_3 in different meteorological conditions and seasons, and in a range of gas phase and aerosol environments, in order to quantify the key processes and pathways of oxidized nitrogen chemistry at night in the troposphere. The ultimate aim was to assess the pervasiveness and importance of nighttime chemical processes, and in particular NO_3, for UK regional and Western European air quality, eutrophication, and ultimately to quantify its links to climate change. The CIMS instrument measured formic acid, propanoic acid, butanoic acid, nitric acid and N_2O_5 during the RONOCO campaign. The BBCEAS measured NO_3, N_2O_5 water and NO_2. 35 hours of data from eight RONOCO flights are presented within this paper for comparison; 5 flights at nighttime in summer 2010, 2 in winter 2011 and 1dusk to dawn transition in winter to study the transition between daytime and nighttime chemistry. All flights sampled air over the UK, North Sea and English Channel which are impacted by pollution from the UK and occasionally continental Europe.

3. Results

3.1. Overall comparison

Figure 5 shows the flight tracks of the aircraft for the data presented within this paper. A typical time series for the BBCEAS and CIMS N_2O_5 data can be seen in figure 6 for flight B566 on January 16th 2011, showing good agreement between the instruments.

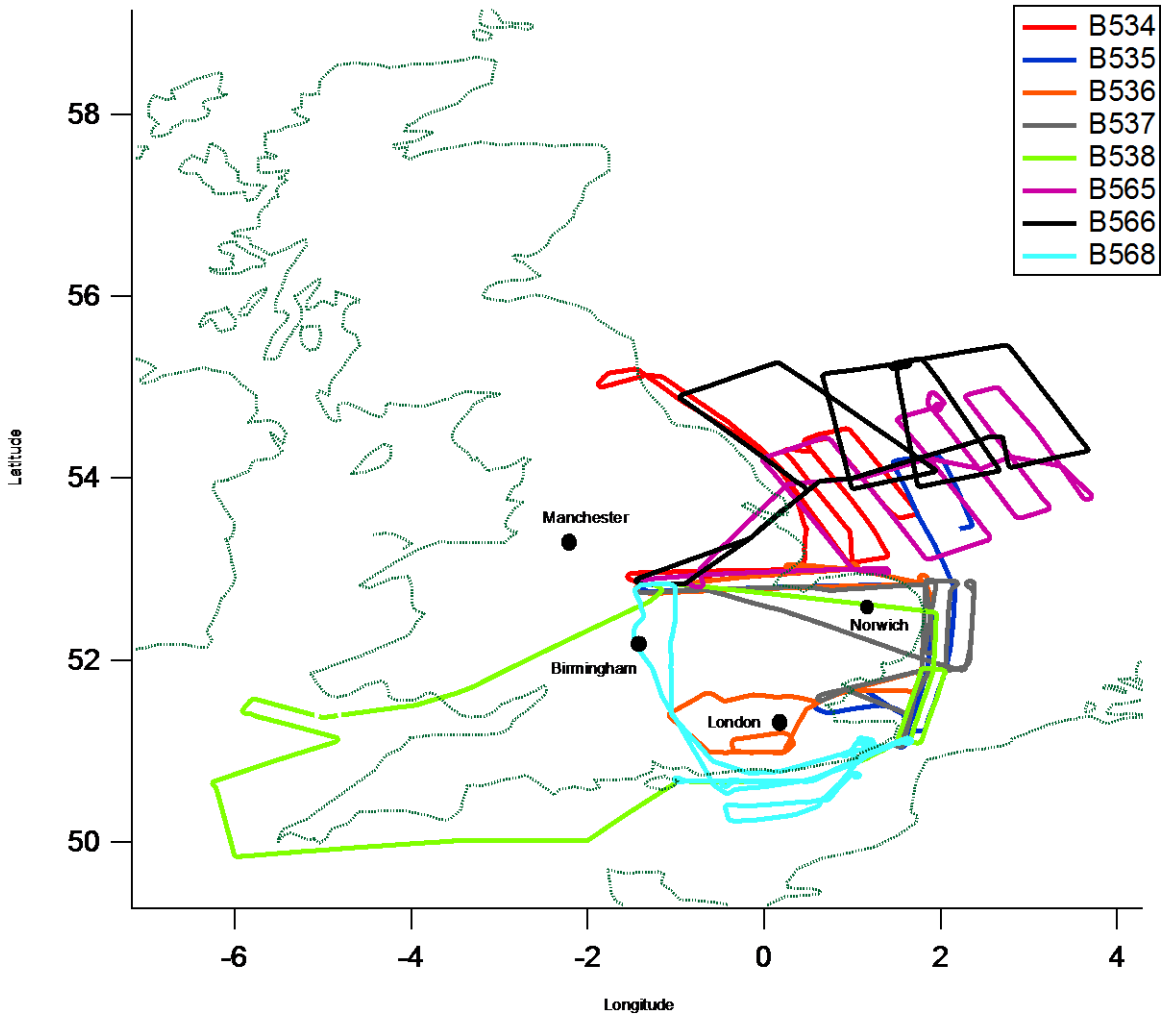

Figure 5. Flight tracks from the RONOCO 2010/2011 campaign for the data presented in this work. Flights B534 to B538 were taken during the summer 2010 campaign and B565 to B568 were taken in January 2011.

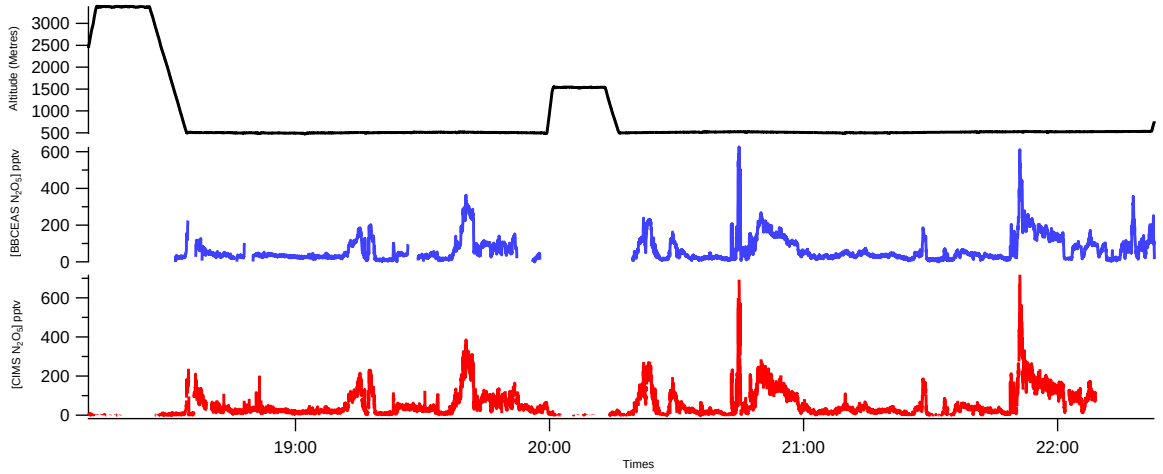

Figure 6. Time series of CIMS (red) and BBCEAS (blue) N_2O_5 concentrations on flight B566 on the 16th January 2011.

The concentrations measured and statistics reported here are at 1 Hz for both instruments. The CIMS sensitivity is calculated as the average sensitivity for the 8 flights presented here. The average sensitivity was 52 ± 2 ion counts $pptv^{-1}s^{-1}$, with a limit of detection of 7.8 pptv, calculated as 3 standard deviations above the background counts, and a total measurement error of 19%. The BBCEAS sensitivity was calculated in Kennedy *et al.* (2011)[13] to be 2.4 pptv for 1 Hz data. Good agreement was obtained between the N_2O_5 measurements using both CIMS and BBCEAS for the 8 flights presented here (top panel of Fig 5). The linear regression exhibits a line of best fit with a correlation coefficient R^2 = 0.89. The agreement between the CIMS and BBCEAS measurements varies from flight to flight as shown in figure 7 and Table 1. Flight B566 has the highest R^2 value of 0.98, whereas as flight B537 has the lowest R^2 of 0.74. This non linearity may be a result of the difference in the instruments method of concentration retrieval. Spectral techniques can be impeded by pressure broadening and interference by water. However the CIMS sensitivity depends on $I.H_2O$ counts, which may decrease at high N_2O_5 concentrations as shown in figure 3. The mean N_2O_5 mixing ratio over the 8 flights presented in this work was 114 pptv for CIMS and 115 pptv for BBCEAS. Maximum concentrations reported by the CIMS and BBCEAS were 890 ± 133 pptv and 1007 ± 141 pptv respectively, although these peak concentrations do not originate from the same air mass. These maxima were intercepted during measurements of the London plume travelling North East over the North Sea, but the BBCEAS maxima was reported during flight B534, whereas the CIMS report the measurement during flight B565.

This discrepancy may arise from the slight curvature in the correlation between the CIMS and BBCEAS for flight B534. An instability of CIMS sensitivity may occur at the high concentrations as a result of the ionisation shifting into a reagent ion dependent regime, therefore causing an inaccuracy in calculating the concentration and subsequently causing the curvature observed. This curvature suggests an underestimation of concentration of N_2O_5 by the CIMS at higher concentrations.

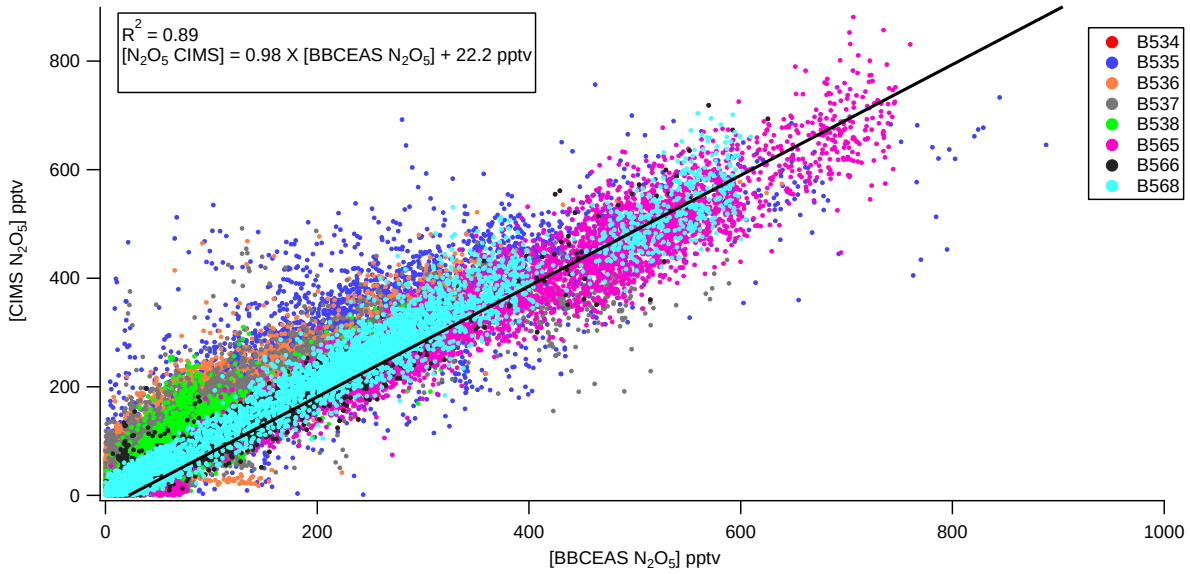

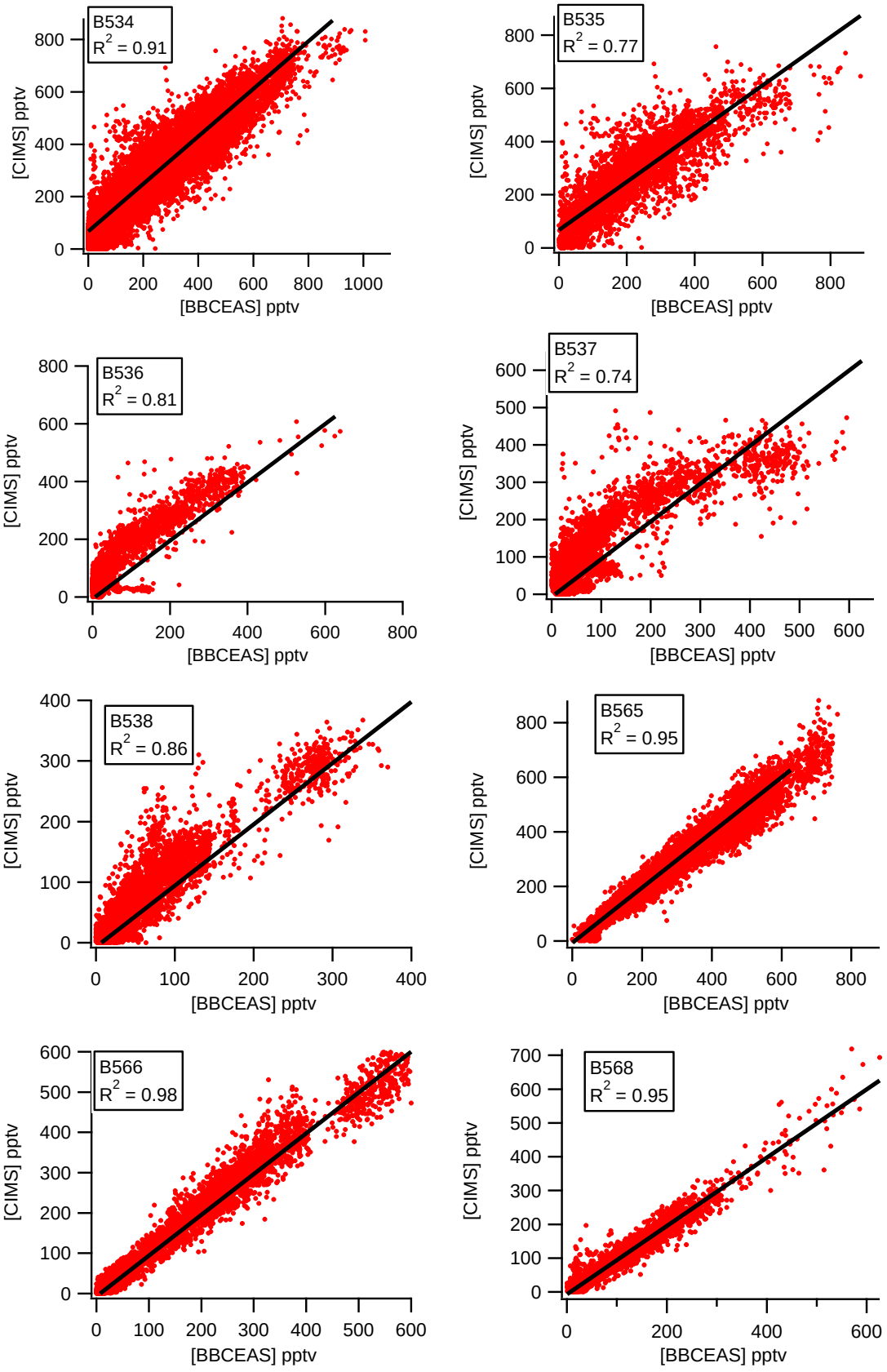
B534
R2 = 0.91
[CIMS] pptv
[BBCEAS] pptv
B535
R2 = 0.77
[CIMS] pptv
[BBCEAS] pptv
B536
R2 = 0.81
[CIMS] pptv
[BBCEAS] pptv
B537
R2 = 0.74
[CIMS] pptv
[BBCEAS] pptv
B538
R2 = 0.86
[CIMS] pptv
[BBCEAS] pptv
B565
R2 = 0.95
[CIMS] pptv
[BBCEAS] pptv
B566
R2 = 0.98
[CIMS] pptv
[BBCEAS] pptv
B568
R2 = 0.95
[CIMS] pptv
[BBCEAS] pptv

Figure 7: Scatter plots for the entire RONOCO dataset accumulated and for each flight from RONOCO where CIMS and BBCEAS measured [N_2O_5]. The black lines illustrate the linear regression.

Table 1. Gradient and error for correlation of CIMS and BBCEAS data for each flight and accumulated flight data.

Flight	slope	error (1 sσ)
All	0.98	0.001
B534	1.00	0.004
B535	0.91	0.007
B536	1.10	0.006
B537	0.91	0.005
B538	1.07	0.005
B565	0.97	0.002
B566	1.01	0.002
B568	1.01	0.002

A previous comparison of N_2O_5 measurements was made by Chang *et al*. (2011)[1] implementing a CRDS and a CIMS sampling ambient air in Boulder, Colorado. An R^2 correlation coefficient of 0.96 was attained for 1 minute averaged data with a gradient for CIMS:CRDS concentrations of 0.76. Although the R^2 for this work (0.89) is slightly lower, the use of 1 Hz data and a gradient of 0.98 shows the robustness of the CIMS and BBCEAS for aircraft measurements

3.2. Comparison as a function of altitude

Vertical profiles obtained from aircraft measurements offer the ability to derive profiles from a variety of air masses, locations and meteorological conditions. Previous profiles obtained from aircraft measurements have shown that concentrations of N_2O_5 are larger and longer lived aloft as compared with the surface[12], as heterogeneous loss of N_2O_5 will generally decrease with altitude[53].

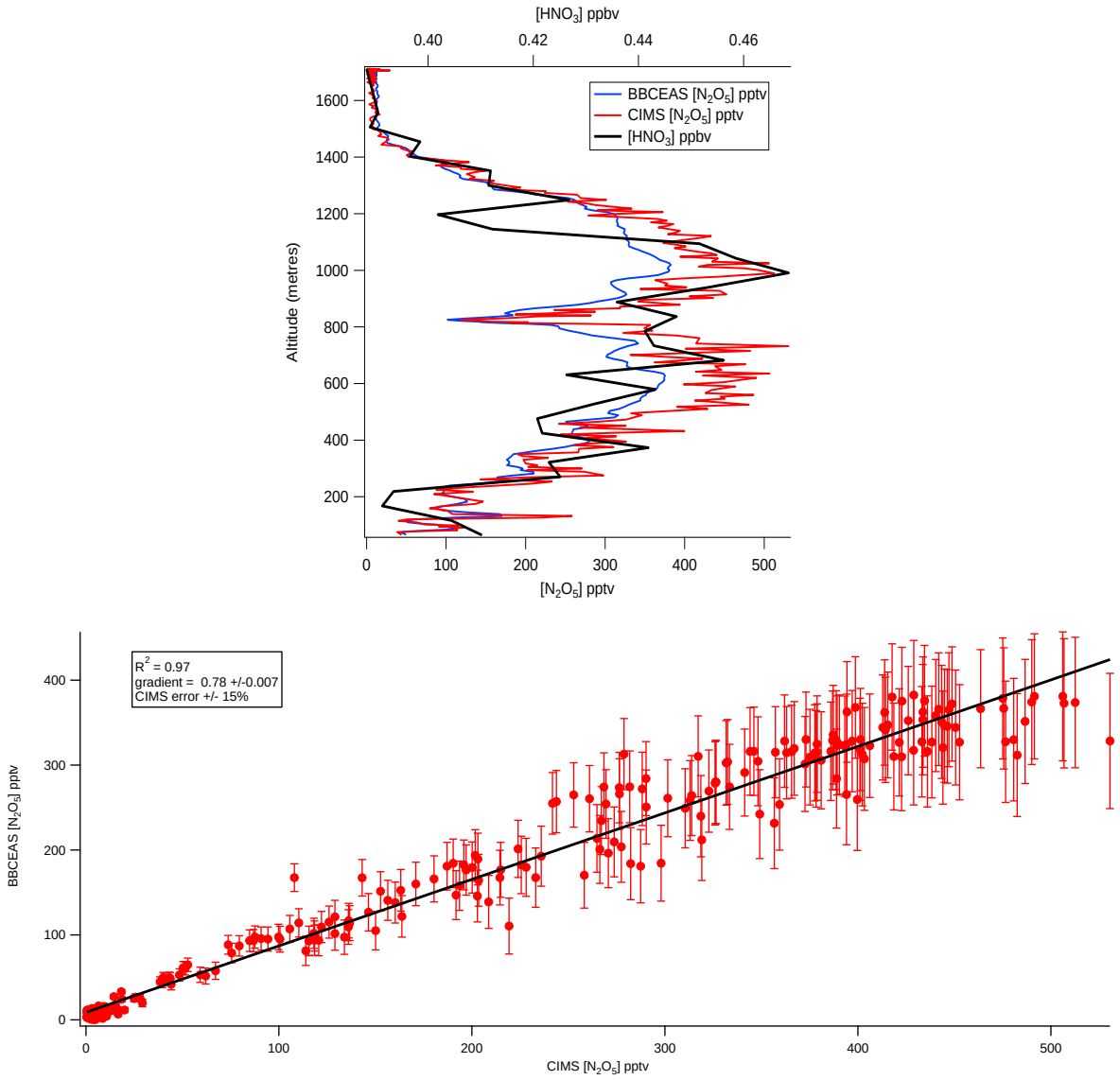

Figure 8: Vertical profiles of N_2O_5 and nitric acid (HNO_3) mixing ratios during a missed approach at Lydd airport, Kent, during B568. The altitude ranges from 64 to 1711 metre. Linear regression line for this data, R^2 = 0.98. HNO_3 measurements are averaged to 15 seconds. The error for CIMS and BBCEAS are 19% and 14% respectively.

Figure 8 illustrates a concentration profile obtained during flight B568, increasing with altitude from 64 metres to 1711 metres. Good agreement between concentrations returned by both instruments, R^2 = 0.98 (as shown in figure 6), confirms the accuracy of the instruments measurements during altitudinal profiles.

At the lowest altitude of 64 metres, both instruments return an average concentration of 45 pptv. A steady increase is observed up to 600 metres where the CIMS records a maximum concentration of 552 pptv and the BBCEAS records a maximum concentration of 353 pptv. Both instruments observe a sharp decrease in N_2O_5 concentration to 100 pptv at 820 metres. An increase again is observed steadily to 300 metres where the CIMS and BBCEAS record concentrations of 512 and 392 pptv respectively. Both instruments observe a very similar drop above this altitude to very small N_2O_5 concentrations (15 pptv) above 1500 metres.

If it is assumed that nitric acid is produced by the hydrolysis of N_2O_5, correlations to the nitric acid profile can aid a comparison between the instruments. Both instruments profiles show a very similar structure to that of nitric acid, although rapid decreases in nitric acid at 200 metres and 1200 metres are not observed in either N_2O_5 measurements. Further analysis using the steady state approximation is presented in a later section.

3.3. Comparison as a function of NO_2

NO_2 plays a key role in nighttime chemistry as it is a primary reactant to N_2O_5 formation; therefore it is useful to observe NO_2 concentrations at the same time as N_2O_5 measurements to understand the N_2O_5 formation and trends. Figure 9 shows the NO_2 data correlated with N_2O_5 concentrations from plume detected during flight B566 at 20:44, which increases above background concentrations during the flight (1.5 ppbv) to 15.7 ppbv. Under these conditions the CIMS and BBCEAS detect a similar increase in N_2O_5 concentrations at this time with close to identical structure. The correlation of N_2O_5 to NO_2 can be seen in figure 9 for the CIMS and BBCEAS which both show a very similar trend (41.82 ± 0.83 pptv N_2O_5 (ppb NO_2)$^{-1}$ for CIMS, 41.10 ± 0.65 pptv ppb^{-1} for BBCEAS) and the same high R^2 value; 0.93. The R^2 for all the data obtained in flight B566 for CIMS and BBCEAS vs NO_2 was 0.59 and 0.62 respectively.

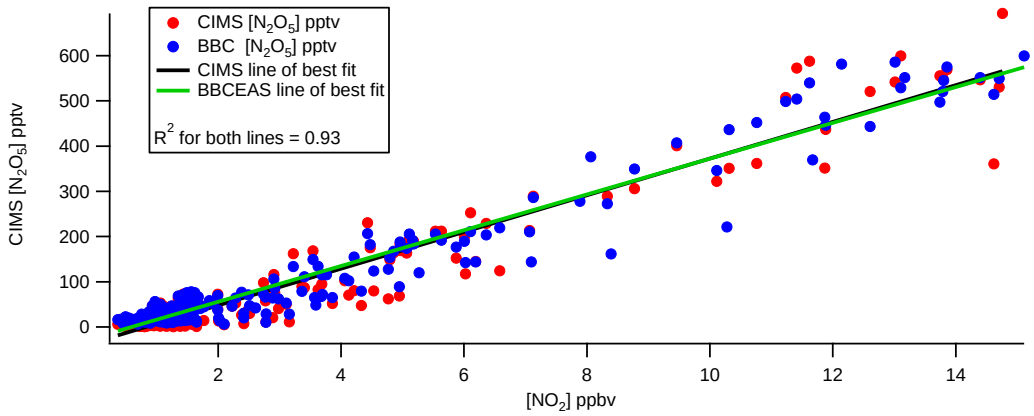

Figure 9: CIMS and BBCEAS N_2O_5 concentration time series during flight B566. NO_2 scatter plot for both N_2O_5 measurements (CIMS in red, BBCEAS in blue) and linear regression line for each (CIMS in black, BBCEAS in green).

3.4. Dusk to nighttime transition flight

Flight B568 took off from East Midlands Airport, Leicestershire, UK at 14:53 on the 19th January 2011 and flew south, operating in the English Channel during the dusk to nighttime transition as observed in figure 10, enabling measurements during daylight and nighttime, enabling observation of the transition from day to nighttime chemistry as sunset was at 16:30. The daytime average N_2O_5 concentrations measured by the CIMS and BBCEAS were 22 ± 3 pptv and 18 ± 3 pptv respectively. An increase in concentration is then observed from the point of sunset, indicating the transition from daytime chemistry to nighttime chemistry. This transition is confirmed by the increasing NO_2 concentration above the earlier background levels, which is expected due to the reduction in photolysis. The high NO_2 concentrations observed from 17:25 until 17:50 correlate with a decrease in O_3 concentrations. Low O_3 mixing ratios are expected and observed to reduce NO_3 and N_2O_5 concentrations. Following the recovery to higher O_3 levels, N_2O_5 and NO_3 progress to their maximum concentrations on the flight. The time series in figure 8 shows that these will originate from the same air mass, but CIMS was calibrating during the time when the BBCEAS measured the maxima and therefore no data could be obtained. This flight shows the ability of both instruments, and measurements of N_2O_5, to track accurately the transition from day to nighttime chemistry and the emergence of NO_2, NO_3 and N_2O_5.

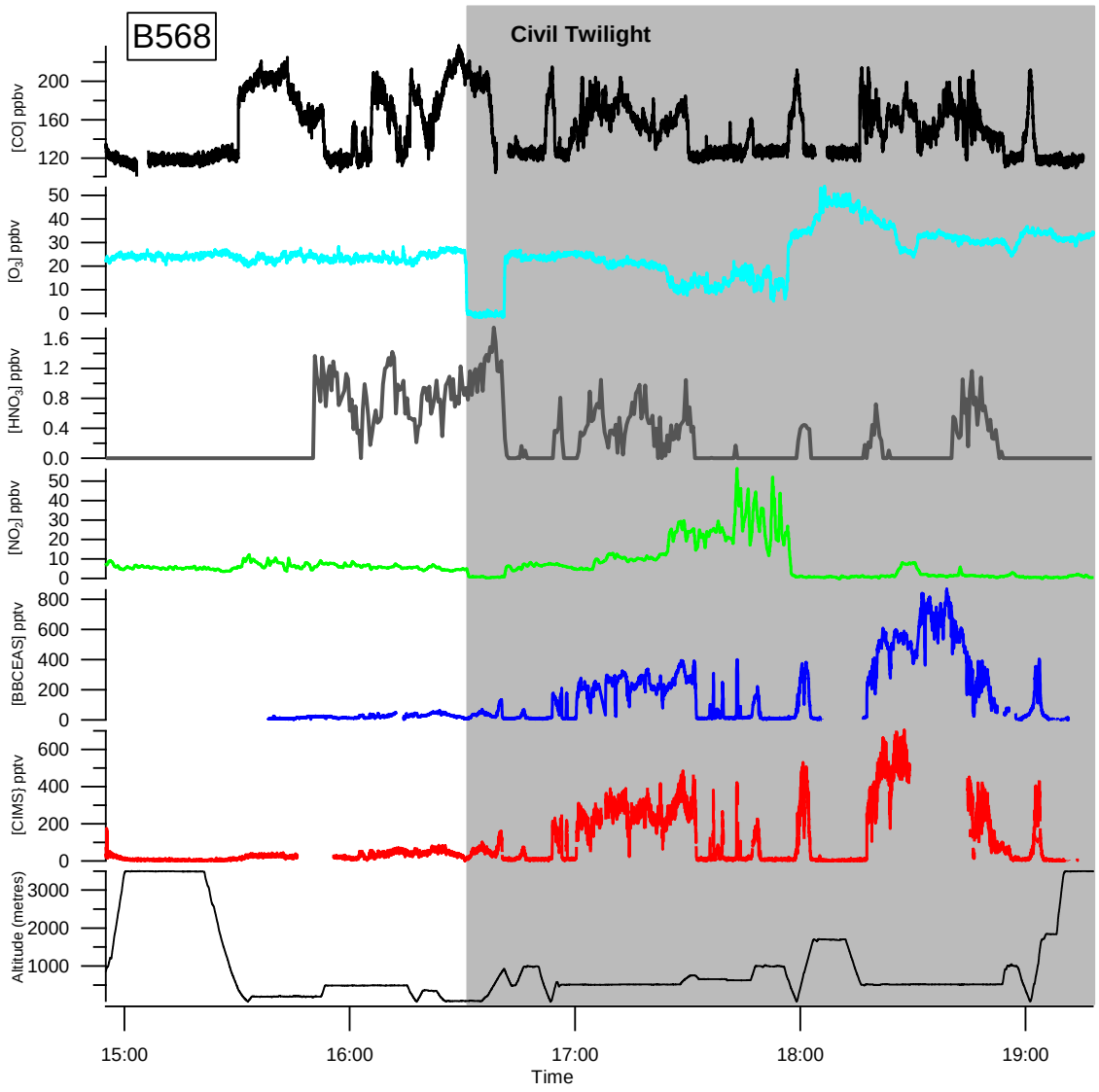
B568
Civil Twilight
[CO] ppbv
200
160
120
[O3] ppbv
50
40
30
20
10
0
[HNO3] ppbv
1.6
1.2
0.8
0.4
0.0
[NO2] ppbv
50
40
30
20
10
0
[BBCEAS] pptv
800
600
400
200
0
[CIMS] pptv
600
400
200
0
Altitude (metres)
3000
2000
1000
15:00
16:00
17:00
18:00
19:00
Time

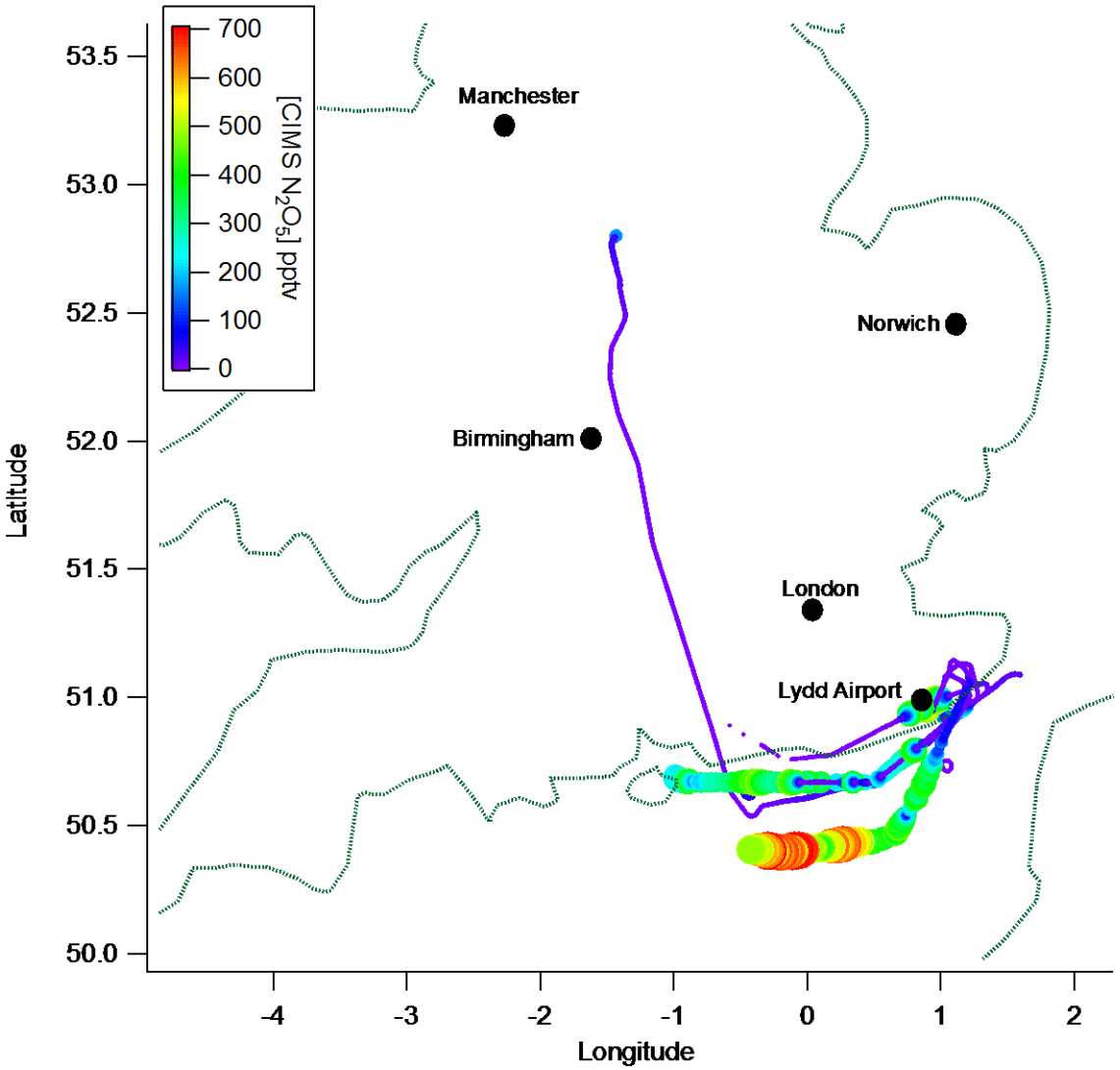

Figure 10: Time series plot and flight track from flight B568 for concentrations of N_2O_5 from the CIMS (red line) and BBCEAS (blue line), NO_2 concentrations (green line) and altitude (black line). A correlation plot of the B568 CIMS and BBCEAS N2O5 data set was shown in the bottom right panel of Fig 5.

4. Steady state analysis

Brown *et al.* (2003)[10] have described in detail the conditions under which the steady state approximation is valid for the analysis of atmospheric levels of NO_3 and N_2O_5. Weak sinks for NO_3 in clean conditions can render the steady state inappropriate and under polluted (e.g large NO_2 concentrations) the equilibrium between NO_3 and N_2O_5 can slow the approach to steady state. We have analysed the dataset presented in this paper and conclude that the

steady state approximation can be applied to the first airborne NO_3 and N_2O_5 measurements over the UK at nighttime during RONOCO. Following the work of Brown *et al.*, (2003)[10] we note that five reactions exist under the conditions encountered that will control both species. These are

$NO_2 + O_3 \rightarrow NO_3 + O_2$ (2)

$NO_3 + NO_2 + M \rightarrow N_2O_5 + M$ (3)

$NO_3 + NO \rightarrow 2NO_2$ (7)

$N_2O_5 + M \rightarrow NO_2 + NO_3 + M$ (8)

$N_2O_5 \rightarrow$ loss (9)

Application of the steady state approximation to NO_3 and N_2O_5 yields the expressions

$$[NO_3] = \frac{k_2[NO_2][O_3]+k_8[N_2O_5][M]}{k_3[NO_2]M+k_7[NO]} \quad \textbf{I}$$

$$[N_2O_5] = \frac{k_3[NO_3][NO_2][M]}{k_8[M]+k_9} \quad \textbf{II}$$

Further manipulations using equations I and II then yield an expression for $[N_2O_5]$ involving just NO, NO_2 and O_3.

$$\frac{k_3[NO_2][M]k_2[NO_2][O_3]}{k_8[M]k_3[NO]+k_9k_3[NO_2][M]+k_9k_7[NO]} = [N_2O_5] \quad \textbf{III}$$

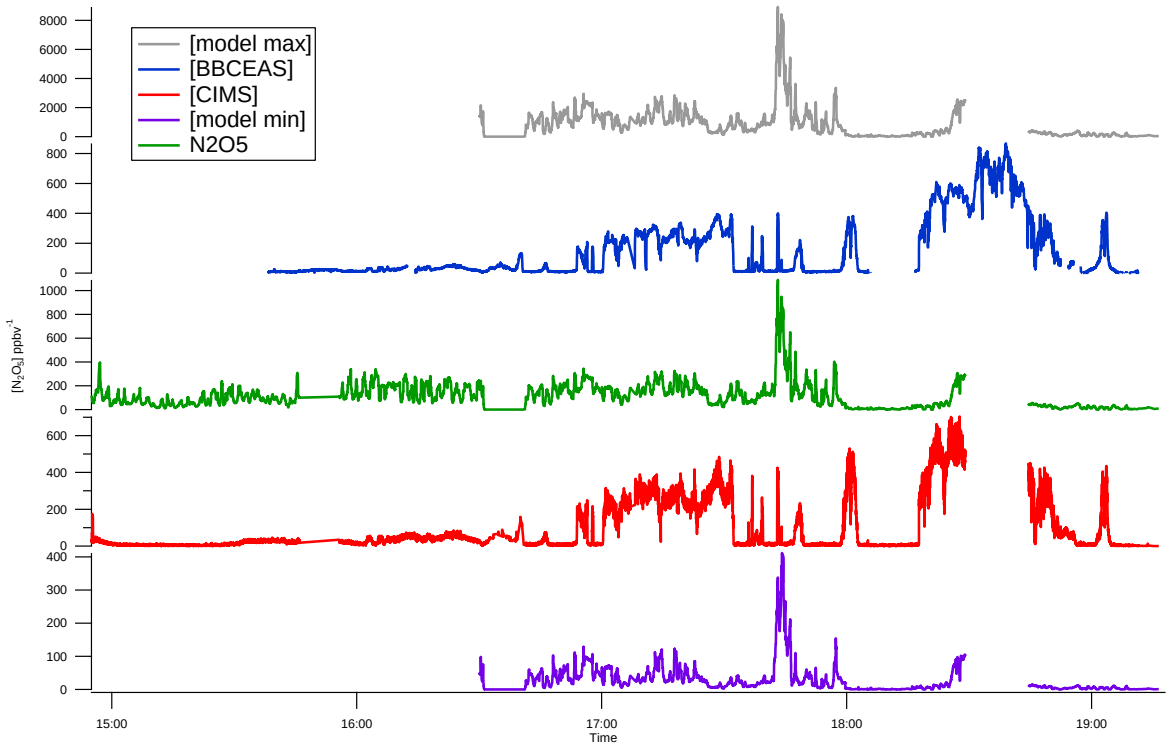

Figure 11: Time series plot from flight B568 of N_2O_5 concentrations from the CIMS (red line) and BBCEAS (blue line) with the results from the model (green line), model minimum (purple line) and model maximum (grey line).

Comparison of the [N_2O_5] derived using equation III using the measurement data of NO, NO_2 and O_3, together with the rate coefficients taken from laboratory studies, with the measured data produces good agreement in general (figure 11). When one includes the combined uncertainties in rate coefficients and species measurements to derive a lower and upper limit for the steady state analysis, these limits easily bracket the measured data. The dataset splits into two regions, one where nighttime NO is large such that NO_3 loss is large via reaction (7). Here, N_2O_5 levels cannot build to high levels and is in keeping with the study by Zheng *et al.*,(2008).[54] These workers studied NO_3 and N_2O_5 vertical profiles during the Milagro campaign over Mexico City and concluded that nighttime NO levels were large and led to a suppression of both species. Alternatively if NO_2 production rate dominates, equation III can be simplified to equation IV which further simplifies to equation V (and is in keeping with the linear correlation between N_2O_5 and NO_2.[10]

$$\frac{k_3[NO_2][M]k_2[NO_2][O_3]}{k_9 k_3[NO_2][M]} = N_2O_5 \qquad \textbf{IV}$$

$$\frac{k_2[NO_2][O_3]}{k_9} = [N_2O_5] \qquad \textbf{V}$$

Rearranging equation V yields an expression for k_9 which involves all parameters that are measured in this work. The range of values returned for flight B568 is ~ from 5 x 10^{-4} s^{-1} to 7 x 10^{-3} s^{-1}, leading to an estimate of the lifetime for N_2O_5 of *ca.* 3 minutes up to about 30 minutes. Assuming that all the N_2O_5 lost produces gas phase HNO_3 (unlikely as one would imagine that a substantial fraction will be incorporated onto aerosol) leads to an upper limit production rate of HNO_3 ~ 30 ppt min^{-1}. Although we note that this is an upper limit, it compares with a typical production rate during daytime through the reaction between OH and NO_2, assuming [NO_2] = 10 ppb, [OH] = 1 x 10^6 molecule cm^{-3}, this produces a production rate of approx. 20 ppt min^{-1}. This result would support the modelling work of Jones *et al.* (2005)[55] who show that the nighttime production of HNO_3 from N_2O_5 chemistry can be an efficient sink for NOx, comparable with the daytime production of HNO_3 from the hydroxyl radical. Daytime and nighttime measurements by Brown *et al.* (2004)[56] also confirm similar $HNOO_3$ production in the daytime and nighttime.

5. Summary and conclusions

The RONOCO campaign 2010/2011 enabled a formal comparison of N_2O_5 concentrations measured by two fundamentally different techniques, CIMS and BBCEAS. The comparison was conducted successfully for the first time on the same aircraft over the UK. The campaign showed how N_2O_5 can be accurately detected at high frequency (1 Hz), with a high sensitivity of 52 ion counts $pptv^{-1}$ with limits of detections down to 2 pptv. Good agreement in general was observed. Linear regression results show that [N_2O_5] CIMS = 0.98 × [N_2O_5] BBCEAS + 22.2 pptv with an average correlation coefficient R^2 = 0.89. The difference between the CIMS and BBCEAS N_2O_5 measurements may be a result of a change in CIMS sensitivity caused by high concentrations of N_2O_5 shifting the ionisation regime into a reagent sensitive scheme. The high correlation during altitudinal profiles (R^2 = 0.93) suggest that the sensitivity of each instrument remains constant throughout varying flight conditions and

allow detailed quick time profiles to be taken in varying environments. Simultaneous NO_2 measurements helped validate the N_2O_5 plumes detected during the campaign and transition from day to night chemistry. These results show that CIMS and BBCEAS techniques can be applied to precise and rapid measurements of N_2O_5 on an aircraft.

Acknowledgments

The authors would like to thank the FAAM staff are also thanked for their assistance in getting the CIMS working onboard the aircraft. The RONOCO consortium was funded by the Natural Environment Research Council, including awards to the universities of Manchester (NE/F004656/1), Cambridge RG50086 MAAG/606 and Leicester (NE/F004761/1). MJSD was supported on a NERC PhD studentship.

References

1 W. L. Chang, P. V. Bhave, S.S. Brown, N. Riemer, J. Stutz and D. Dabdub, D, Aerosol Sci. Technol, 2011, **45**, 665–695, doi:10.1080/02786826.2010.551672

2 S. S.Brown, J. Stuts, J, Chem. Soc. Rev, 2012, **41**, 19, 6405-6447, doi: 10.1039/C2CS35181A

3 F. J. Dentener and P. J. Crutzen , J. Geophys. Res, 1993, **98**, 7149–7163.

4 H. S. Johnston, Science, 1971, **173,** 517–522.

5 R. Atkinson, and J. Arey, Atmos. Environ, 2003, **37**, S197–S219.

6 H. Osthoff, J. M. Roberts, A. R. Ravishankara, E. J. Williams, B. M. Lerner, R. S. Sommariva, T. S. Bates, D. Coffman, P.K. Quinn, J. E. Dibb, H. Stark, J. B. Burkholder, R. K. Talukdar, J. Meagher, F. C. Fehsenfeld and S. S. Brown, Nat. Geosci., 2008, **1**, 324–328, doi:10.1038/ngeo177.

7 S. S. Brown, W. P. Dub´ e, H. D. Osthoff, J. Stutz, T. B. Ryerson, A. G. Wollny, C. A. Brock, C. Warneke, J. A. de Gouw, E. Atlas, J. A. Neuman, J. S. Holloway, B. M. Lerner, E. J. Williams, W. C. Kuster, P. D. Goldan, W. M. Angevine, M. Trainer, F. C. Fehsenfeld and A. R. Ravishankara, J. Geophys. Res., 2007a, **112**, D22304, doi:10.1029/2007JD008883.

8 R. J. Atkinson, Phys. Chem. Ref. Data, 1991, **20**,459–507.

9 R. Atkinson, Atmos. Environ, 2000, **34**, 2063–2101.

10 S. S. Brown, H. Stark and A. R. Ravishankara, J. Geophys. Res.-Atmos, 2003, **108**(D17), 4539, doi:10.1029/2003JD003407.

11 H. Stark, B. M. Lerner, R. Schmitt, R. Jakoubek, E. J. Williams, T. B. Ryerson, D. T. Sueper, D. D. Parrish and F. C. Fehsenfeld, J. Geophys. Res-Atmos, 2007, **112**(D10S04), doi:10.1029/2006JD007578.

12 S. S. Brown, W. P.Dub´ e, H. D. Osthoff, D. E. Wolfe, W. M. Angevineand A. R. Ravishankara, Atmos. Chem. Phys, 2007b, **7**, 139–149, doi:10.5194/acp-7-139-2007.

13 O. J.. Kennedy, B. Ouyang, J. M. Langridge, M. J. S. Daniels, S. Bauguitte, R. Freshwater, M. W. McLeod, C. Ironmonger, J. Sendall, O. Norris, R. Nightingale, S. M. Ball, and R. L. Jones, Atmos. Meas. Tech., 2011, **4**, 1759-1776, doi:10.5194/amt-4-1759-2011.

14 E. D. Morris and H. J. Niki, Phys. Chem, 1973, **77**:1929–1932.

15 M. Mozurkewich and J. G. Calvert, J. Geophys. Res, 1988, 93:15889–15896.

16 N. Riemer, H. Vogel, B. Vogel, B. Schell, I. Ackermann, C. Kessler and H. Hass, J. Geophys. Res, 2003, **108**, 4144,doi:10.1029/2002jd002436.

17 S. S. Brown and J. Stutz, Chem. Soc. Rev, 2012, **41**, 19, 6405-6447, doi: 10.1039/C2CS35181A.

18 A. W. Stelson and J. H. Seinfeld, Atmospheric Environment, 1982a, **16 (**5), 983–992.

19 A. G. Russell and G. R. Cass, Atmos. Environ, 1986, **20**,10, 2011-2025.

20 D. Lillis, C. N. Cruz, J. Collett, L. W. Richards and P. N. Pandis, Atmos. Environ, 1999, **33:**4797–4816, 1999.

21 S. Yu, R. Dennis, S. Roselle, A. Nenes, J. Walker, B. Eder, K. Schere and J. Swall, J. Geophys. Res., 2005, **110**:D07S13.

22 H. P. J. Liao, S. H. Adams, J. H. Chung, L. J. Seinfeld, D. J. Mickley and J. Jacob, J. Geophys. Res., 2003, **108**, D1, 4001, doi:10.1029/2001JD001260.

23 Y. Feng and J. E. Penner, J. Geophys. Res. 2007, **112**:D01304. doi: 10.1029/2005JD006404.

24 S. E. Bauer, D. Koch, N. Unger, S. M. Metzger, D. T. Shindell and D. G. Streets, Atmos. Chem. Phys, 2007, **7**:5043–5059.

25 S. S. Brown, J. A. Neuman, T. B. Ryerson, M. Trainer, W. P. Dub´ e, J. S. Holloway, C. Warneke, J. A. D. Gouw, S. G. Donnelly, E. Atlas, B. Matthew, A. M. Middlebrook, R. Peltier, R. J. Weber, A. Stohl, J. F. Meagher, F. C. Fehsenfeld and A. R. Ravishankara, Geophys. Res. Lett., 2006 **33**, L08801, doi:10.1029/2006GL025900.

26 T. H. Bertram and J. A. Thornton, Atmos. Chem. Phys, 2009, **9,** 8351–8363, doi:10.5194/acp-9-8351-2009, 2009.

27 U. Platt, D. Perner, A. M. Winer, G. W. Harris and J. N. Pitts, Geophys. Res. Lett., 1980, **7**(1), 89–92.

28 A. B. Geyer, S. Alicke, T. Konrad, J. Schmitz, U Stutz, and S. Platt, J. Geophys. Res., 2001, **106**, 8013–8026, 2001.

29 N. Smith, J. M.C. Plane, C. F., Nien and P.A. Solomon P A, *Atmos Environ*, 1995, **29**: 2887–2897.

30 S. S. Brown, W. P. Dub´ e, H. D. Osthoff, J. Stutz, T. B. Ryerson, A. G. Wollny, C. A Brock, C. Warneke, J. A. de Gouw, E. Atlas, J. A. Neuman, J. S. Holloway, B. M. Lerner, E. J. Williams, W. C. Kuster, P. D. Goldan, W. M. Angevine, M. Trainer, F. C. Fehsenfeld and A. R. Ravishankara, J. Geophys. Res., 2007a, **112**, D22304, doi:10.1029/2007JD008883.

31 W. P. Dub´ e, S. S. Brown, H. D. Osthoff, M. R. Nunley, S. J. Ciciora M. W. Paris, R. J. McLaughlin, A. R. Ravishankara, Rev. Sci. Instrum, 2006, **77**(3), 034101– 034101-11, doi:10.1063/1.2176058.

32 D. L. Slusher, L. G. Huey, D. J. Tanner, F. M. Flocke and J. M. Roberts, J. Geophys. Res.-Atmos, 2004, **109**, D19315, DOI: 10.1029/2004JD004670.

33 J. Matsumoto, H. Imai, N. Kosugi and Y. Kaji, Atmos. Environ., 1995, **39**, 6802–6811.

34 E. C. Wood, P. J. Wooldridge, J. H. Freese, T. Albrecht and R. C. Cohen, Environ. Sci, 2003, 30 Technol., **37**, 5732–5738, doi:10.1021/es034507w.

35 H. P. Dorn, R. L. Apodaca, S. M. Ball, T. Brauers, S. S. Brown, J. N. Crowley, W. P. Dube, H. Fuchs, R. Haseler, U. Heitmann, R. L. Jones, A. Kindler-Scharr, I. Labazan, J. M. Langridge, J. Meinen, T. F. Mentel, U. Platt, D. Pohler, F. Rohrer, A. A. Ruth, E. Schlosser, G. Schuster, A. J. L. Shillings, W. R Simpson, J. Thieser. R. Tillmann, R. VArma, D. S. Venables and A. Wahner, Atmos. Meas. Tech, 2013, **5**, 1111-1140 DOI:10.5194/amt-6-1111-2013.

36 S. S. Brown, Chem. Rev, 2003, **103**, 5219–5238, doi:10.1021/cr020645c.

37 S. E. Fiedler, A. Hese and A. A. Ruth, Chem. Phys. Lett., 2003, **371**, 284–294, doi:10.1016/s0009-2614(03)00263-x.

38 T. Gherma, D. S. Venables, S. Vaughan, J. Orphal and A. A. Ruth, Environ. Sci. Tech., 2008, **42**, 3, 890-895, doi: 10.1021/es0716913, 2008.

39 R. A. Washenfelder, A. O. Langford, H. Fuchs and S. S. Brown, Atmos. Chem. Phys., **8**, 2008, 7779-7793, doi:10.5194/acp-8-7779-2008, 2008.

40 U. Platt, J. Meinen, D. Poehler, and T. Leisner, Atm. Meas. Tech., 2009, **2**, 713-723.

41 T. Wu, W. Zhao, W. Chen, W. Zhang, and G. Gau, G, App. Phys. B-Las. Opt, 2009, **94**, 1, 85-94, doi: 10.1007/s00340-008-3308-8,.

42 R. Thalman and R. Volkamer, Atmos. Meas. Tech., 2010, **3**, 1797-1814, doi:10.5194/amt-3-1797-2010.

43 S. B. Darby, P. D. Smith, P. D and D. D. Venables, Analyst, 2012, **137**, 2318–2321.

44 J. M. Langridge, S. M. Ball, A. J. L. Shillings and R. L. Jones, Rev. Sci. Instrume, 2008, **79**, 123110, doi:10.1063/1.3046282.

45 A. K. Benton, J. M. Langridge, S. M. Ball, W. J. Bloss, M. Dall'Osto, E. Nemitz, R. M. Harrison and R. L. Jones, Atmos. Chem. Phys., 2010, **10,** 9781-9795, doi:10.5194/acp-10-9781-2010.

46 D. J. Tanner, F. L. Eisele, J. Geophys. Res, 1991, **96**:1023.

47 L. G. Huey, Mass. Spec. Rev., 2007, **26**, 166-84.

48 J. B. Nowak, J. A. Neuman, K. Kozai, L. G. Huey, D. J. Tanner, J. S. Holloway, T. B. Ryerson, G. J. Frost, S. A. McKeen and F. C. Fehsenfeld, J. Geophys. Res.-Atmos, 2007, **112**, D10S02, DOI:10.1029/2006JD007589, 2007.

49 M. Le Breton, M. R. Mcgillen, J. B. A. Muller, A. Bacak, D. E. Shallcross, P. Xiao, L. G. Huey, D. Tanner, H. Coe and C. J. Percival, Atmos. Meas. Tec, 2012, **4**, 5807-5835.

50 M. Le Breton, A. Bacak, J. B. A. Muller, P. Xiao, B. M. A. Shallcross, R. Batt, M. C. Cooke, D.E. Shallcross, S.J-B. Bauguitte and C. J. Percival, Atmos. Environ, 2013, **83**, 166-175.

51 D. J. Stewart, C. M. Taylor, C. E. Reeves and J. B. McQuaid, Atmos. Chem. Phys., 2008, **8**, 2285-2297.

52 E. Real, K. S. Law, B. Weinzierl, M. Fiebig, A. Petzold, O. Wild, J. Methven, S. Arnold, A. Stohl, H. Huntrieser, A. Roiger, H. Schlager, D. Stewart, M. Avery, G. Sachse, E. Browell, R. Ferrare and D. Blake, J. Geophys. Res.-Atmos., 2007, **112**, D10S41, doi:10.1029/2006JD007576.

53 D. J. Fish, D. E. Shallcross and R. L. Jones, Atmos. Environ., 1999, **33**, 687-691.

54 J. Zheng, R. Zhang, E. C. Fortner, R. M. Volkamer, L. Molina, A. C. Aiken, J. L. Jiminez, K. Gaeggeler, J. Dommen, S. Dusanter, P. S. Stevens and X. Tie, Atmos. Chem. Phys., 2008, **8**. 6823-6838.

55 R. L. Jones, S. M. Ball, and D. E. Shallcross, Faraday Discuss., 2005, **130**, 165–179, doi:10.1039/b502633b.

56 S. S. Brown, J. E. Dibb, H. Stark, M. Aldener, M. Vozella, W. Whitlow, E. J. Williams, B. M. Lerner, R. Jakoubek, A. M. Middlebrook, J. A. DeGouw, C. Warneke, P. D. Goldan, W. C. Kuster, W. M. Angevine, D. T. Sueper, P. K. Quinn, T. S. Bate, J. F. Meagher, F. C. Fehsenfeld and A. R. Ravishankara, Geophys. Res. Lett, 2004, **31**, L07108.